Research article

SURFACE and INTERFACE ANALYSIS

Received: 11 December 2014 Revised: 16 March 2015 Accepted: 18 March 2015 Published online in Wiley Online Library

(wileyonlinelibrary.com) DOI 10.1002/sia.5770

# Behavior of nitrided and carburized AISI 904L stainless steels under severe light ion beam irradiation with plasma focus

J. García Molleja,[a,b]* M. Milanese,[c] B. J. Gómez,[b] R. Moroso,[c] M. Piccoli,[d] J. Niedbalski,[c] J. Bürgi,[b] E. Bemporad[d] and J. Feugeas[b]

**Superaustenitic stainless steels have become of growing interest in industrial and technological fields, but there is not a complete understanding on their fundamental properties and their performances. For this paper, AISI 904 L superaustenitic samples were nitrided and carburized in order to study the expanded austenite stability under severe deuterium and helium ion bombardment. Surface treatments were conducted using pulsed plasma glow discharges in a low pressure atmosphere, and a dense plasma focus device was used to irradiate the samples. Characterization techniques used were focused ion beam/SEM, energy-dispersive X-ray spectroscopy, and grazing incidence X-ray diffraction. Our results showed in carburized samples lattice expansion growth with the time treatment, but in nitrided samples, an expanded austenite reduction with time treatment was observed due to the formation of nitride nanoagglomerates. Moreover, this ion impingement provoked surface melting and a severe collision cascade, and a damaged bead located under the craters composed solely of minor alloying atoms. Furthermore, nitrided samples were more stable following ion bombardment than the carburized ones. When helium ions were used, the loss of expansion (triggered by diffusion processes of N or C to deeper regions) was more pronounced in the expanded austenite, but when deuterium ions were used to bombard the sample, there was a crystallite development of stressed austenite, which provoked a diffraction peak arousal at 43.3°. Copyright © 2015 John Wiley & Sons, Ltd.**

**Keywords:** ion carburizing; ion nitriding; expanded austenite; superaustenitic stainless steels; plasma focus; crystalline stability

## Introduction

Austenitic stainless steels have been applied for industrial purposes because of the excellent properties that these materials have,[1] like good corrosion resistance to chloride pitting, great hygiene/cleanliness factor, easy transformation, good welding properties, no hardening after heat treatment, and resistance to high and low temperatures. Moreover, in recent years, applications in the industrial field of superaustenitic stainless steels, like AISI 904 L grade, have increased.[2,3] Mechanical, physical, and chemical properties of these steels are unique because of the low carbon content and the high proportion of nickel, chromium, molybdenum, and copper[4] elements. Mainly, the superiority of these superaustenitic stainless steels lies in their good weldability and great resistance to pitting and crevice corrosion and good mechanical strength.[5] This high resistance to stress, corrosion, and cracking is obtained by the high amount of Ni in their structure, while Mo and N improve the pitting and crevice corrosion resistance.[2] Indeed, Fernandes *et al.*[5] say that N is responsible for austenite phase stabilization and acts as a suppressor of intermetallic phases.

However, in order to improve the hardness and wear resistance in both austenitic and superaustenitic steels without change of any other properties, the development of expanded austenite has been devised.[6,7] This phase is the result of nitrogen or carbon atoms entering a face-centered cubic (fcc) crystalline structure until colossal supersaturation is reached[8,9] when a high number of these atoms occupy the fcc interstitial sites. Because of this process, the deformation of crystalline structure by compressive strains and high density of stacking faults is observed, which induces lattice parameter growth.

Ion nitriding[10] and carburizing[11] using low-pressure cold plasma are techniques based on surface modification that are applied to obtain expanded austenite through N or C diffusion in the lattice, respectively. Under low current densities, the expanded austenite formed has no nitride or carbide precipitation, so the steel surface has an improvement of hardness and wear resistance, well above that of the original material.

The stability of expanded austenite is an interesting problem due to the huge range of conditions where austenitic and superaustenitic stainless steels can be applied. For example, superaustenitic steels

* *Correspondence to: J. García Molleja, Institut des Matériaux Jean Rouxel, IMN – Université de Nantes, UMR CNRS 6502, 2 rue de la Houssinière, Nantes, 44322, Cedex 3, France.*
*E-mail: javier.garcia-molleja@cnrs-imn.fr*

a *Institut des Matériaux Jean Rouxel, IMN – Université de Nantes, UMR CNRS 6502, 2 rue de la Houssinière, Nantes 44322, Cedex 3, France*

b *Instituto de Física Rosario (CONICET – UNR), 27 de Febrero 210 bis, Rosario S2000EZP, Argentina*

c *Instituto de Física Arroyo Seco (CONICET – UNICEN), Pinto 399, Tandil B7000GHG, Argentina*

d *Department of Engineering, University of Rome 'Roma TRE', Via della Vasca Navale 79, Rome 00146, Italy*

are used in nuclear technology as clad inner walls of the reactor and fuel wrappers in fast breeder reactors[12], in which the material is strongly irradiated.[13] The role of expanded austenite acting as first wall in nuclear fusion devices (i.e. Tokamak, International Thermonuclear Experimental Reactor (ITER)) has been poorly studied. In these devices, deuterium (D) is the most used fuel and helium (He) is a typical byproduct after a D + D reaction. Furthermore, He is obtained when the nuclear reaction is induced by D and tritium (T) and after T regeneration when for this purpose, neutrons and lithium are used.

Fusion reactors use high-energy deuteron beams and hot and fast D plasma jets. Besides, He nuclei, neutrons, and tritons have high energy after the nuclear reaction, so the reactor first wall is always under severe bombardment. The ITER divertor region is a clear example of this environment. In order to simulate these low activation materials submitted to a high bombardment of light ions, a dense plasma focus (DPF) configuration, like Rico or PACO configurations, for example, could be used.[14,15] Plasma focus can use other light elements, like N or C, but in nuclear fusion, these ions are not present, only D, He, neutrons, and T. Moreover, if after light ion bombardment, C or N from the expanded austenite is released, they do not affect the nuclear reaction region. Furthermore, they are not transformed in ions impinging the first wall.

Therefore, this paper goes a step beyond the scope developed in the work of García Molleja[16] and is mainly focused on the surface modification and performance of a selected material. For this paper, AISI 904 L stainless steel was chosen in order to develop, in its surface, the phase called expanded austenite, which was obtained by ion nitriding and ion carburizing. Although AISI 904 L has an increasing interest in industry, there are no studies focused on its surface modification using cold plasmas. Thus, this paper presents novel results regarding the development of expanded austenite using N or C atoms. Moreover, these treated samples were submitted to an intense bombardment[17] of helium and deuterium ions (simulating the first wall in a nuclear reactor) using a plasma focus device[18] in order to study the stability according to the surface treatment used. DPF is customarily used to simulate the stability of materials acting as first wall in a nuclear reactor although the use of tritium is avoided because of the extreme difficulty (and high costs) of handling this gas. Again, the analysis of the stability of AISI 904 L steel under ion irradiation after expanded austenite development is primarily accomplished for this paper. The effects of the ion irradiation and the heat treatment induced were clarified, and the gradual degradation of expanded austenite was measured.

## Experimental

### Sample preparation

Samples were obtained from a 20-mm-diameter AISI 904 L bar, whose elemental composition is consigned in Table 1. Samples had a thickness of 6 mm in order to enable the right placement in the sample holder. Samples surfaces were polished until mirror appearance. The process ended with lathing with an emulsion containing 1-μm alumina powder in suspension. Before the treatment process, surfaces were cleaned with alcohol and acetone and dried with hot air.

### Surface modification with plasma glow

In this work, a 5.1-l capacity reactor made of AISI 304 L stainless steel was used. The cathode with several holes to place the steel samples in was described elsewhere.[16] It is worth mentioning that its shape avoids the sharp edge effect of electric discharges during the process.[19] High-purity gases were employed for plasma treatment, and they were inserted 9 cm above the cathode through a Pyrex glass pipe.

Base pressure was ~ $10^{-3}$ mbar, and $H_2$ cleaning plasma was used for 15 min to eliminate mainly the remaining water adsorbed on samples and internal walls of chamber. After that, a heating process was implemented consisting of a plasma generation of 80% of $H_2$ and 20% of Ar gas mixture until samples reach the working temperature, i.e. 390–400 °C. Once the heating process was finished, the atmosphere was changed to 80% $H_2$–20% $N_2$, which is the processing atmosphere, always at 5 mbar for 40 and 80 min of processing. For comparative purposes, some samples were carburized under a gas mixture of 5% $CH_4$/45% $H_2$/50% Ar at 5 mbar.

Glow plasma was maintained with a pulsed-direct current (DC) generator with square wave and frequency of 100 Hz.[20] Duty cycle was adjusted to 2 : 3 (off : on cycle), and this power supply was connected to a load resistance of 140 Ω. In Table 2, it is possible to see the experimental conditions used during the nitriding and carburizing processes.

### Pulsed ion beam

Irradiation effect on expanded austenite was performed by the ion beams accelerated in DPF discharges.[21] The DPF unit used was a 2-kJ Mather type with 40-mm free length electrodes, consisting of a coaxial pipe configuration with a 40-mm-diameter anode, a 15-mm long Pyrex insulator, and a cathode made up of 12 bars disposed on a 100-mm-diameter circumference.

This Z-pinch experiment[14] under an atmosphere of 1.643 mbar of high-purity deuterium or helium consisted of a fast discharge between electrodes generating in the end a high density plasma column in front of the anode and along the symmetry axis of the coaxial electrode system,[22,23] accelerating ions to the front, where the samples were located at 82 mm of distance. The energy of the ions in the beams had a continuous spectrum ranging between 30 and 500 keV.

**Table 2.** Nitriding and carburizing experimental parameters used in the samples with plasma glow pulsed-DC discharge under controlled atmosphere

| | p (mbar) | V (V) | I (A) | j (mA/cm$^2$) | T (°C) |
|---|---|---|---|---|---|
| Nitriding | 5.012 | 541 | 0.911 | 3.43 | 404 |
| Carburizing | 4.993 | 475 | 1.053 | 3.97 | 388 |

**Table 1.** Elemental composition (in at.%) of AISI 904 L substrate used in this work

| Steel | C | Si | Mn | Ni | Cr | Mo | Cu | N | S | P | Fe |
|---|---|---|---|---|---|---|---|---|---|---|---|
| 904 L | 0.02 | 0.64 | 1.53 | 24.04 | 19.27 | 4.21 | 1.30 | 0.04 | 0.0006 | 0.022 | Balance |

Under such an experimental configuration, surfaces receive an ion beam pulse with a fluence of ≈ $10^{13}$–$10^{14}$ $cm^{-2}$ with pulse duration of ≈ 400 ns,[24] delivering on the surface a density power of 10 MW/$cm^2$.[25] Thus, this energy transfer resulted in a fast temperature increase during this time interval up to thousands of degrees,[26] followed by fast cooling by thermal conduction to the sample bulk, reaching room temperature in tens of microseconds.[18] In this paper, one pulse per second was utilized, reaching a total number of 20 pulses. It is worth mentioning that all operational conditions in the plasma focus device were the same for each treated sample.

### Characterization techniques

*X-ray diffraction*

Crystal structure and lattice parameters were studied using the X-ray diffraction technique in the grazing incidence mode (GIXRD) with a PHILIPS X'Pert device (Royal Philips Ltd., Amsterdam, Netherlands) with a $CuK_{\alpha 1}$ radiation ($\lambda = 1.54056$ Å) with a $4 \times 4$ $mm^2$ cross section parallel incident X-ray beam and with an angular diffraction detector variation of 0.03° every step with accumulating time of 1 s. Incidence was 10°, and diffraction angle varied between 30° and 80°.

*Focused ion beam/SEM analyses*

The surface layer structure was investigated through focused ion beam (FIB)/SEM. FIB analysis was achieved with an FEI Helios NanoLab™ 600 (Dualbeam) device (FEI Company, Hillsboro, Oregon, USA), which has a $Ga^+$ beam.[27] On FIB images, the degree of gray observed in the cross section originated because of the efficiency of secondary electrons, the depth where the interaction occurs, and the type of atom. SEM mode can be obtained in this device by primary electron emission. When the crater is created, FIB images are taken at 30 kV and 28 pA, and SEM images are taken at 5 kV and 0.17 nA. The sample can be tilted up to 52° to observe both surface and cross section. Indeed, this device could obtain energy-dispersive X-ray spectroscopy (EDS) profiles using a map mode in order to detect the element presence or absence.

## Results and discussion

### Nitrided and carburized layers

For comparative purposes, the lattice parameter of the base material was measured using the GIXRD technique: AISI 904 L had a constant of 3.6009 Å. The higher Ni concentration in AISI 904 L steels develops higher lattice parameters in comparison with the AISI 300 series, for example, in the works of García Molleja *et al.*[11] and Baldenebro-López *et al.*[28] According to Nascimento *et al.*[29] in their analysis of the two important stainless steels in industry, AISI 316 grade has a parameter lattice of 3.5935 Å, and AISI 304 steel has a value of 3.5918 Å.

After the nitriding process, clear behaviors in the two time treatments used (40 and 80 min) were detected. Diffraction peaks were shifted to lower angular values because of the addition of nitrogen atoms in the interstitial sites and the expansion of the crystal structure. This new phase is known as expanded austenite.[7,11] It is important to mention that after 40 min of nitriding, the (111) peak was located at lower angular values than the same peak obtained when the nitriding process was 80 min of duration. That is, at 40-min nitriding, the relative expansion was 6.12%, but this value decreased to 5.04% in samples nitrided for 80 min (Fig. 1a).

In principle, more time treatment means more expanding elements in the lattice and higher structure distortion, but at some nitrogen concentrations, formation of nitrides could be triggered,[30] stealing the excess of nitrogen in order to form these compounds and developing the loss of expansion measured.[31] Indeed, nitrides were not detected by GIXRD, but it is probable that the nitride was precipitated by nanoagglomerates in the very surface, so the difficulty of measuring them is high.[32] A possible technique in order to verify the formation of these nanoagglomerates could be the analysis of surface corrosion using potentiodynamic polarization.[19,33] Furthermore, nanoindentation is another technique focused on the detection of these nanoagglomerates of nitrides/carbides because the hardness of these regions must be superior as regards their surroundings. Detailed FIB/SEM analyses with EDS could serve as a detector of nanoagglomerates too.

On the other hand, carburized samples, shown in Fig. 1b, did not present this behavior. There was a peak shifting that revealed the formation of the expanded austenite phase, but this expansion was higher after 80 min of treatment (relative expansion of 4.76%) than after 40 min of treatment (relative expansion of 4.41%). This behavior can be explained by the different values of solubility in the fcc crystalline phase and the consequent high mobility of the carbon atoms to higher depths.[34]

Furthermore, this difference in atom solubility in the austenite structure was responsible for the differences in total expansion obtained between the carburizing process and the nitriding one.[35] When samples treated for the same time durations are compared, nitrided ones (3.8214 Å for 40 min) had higher lattice parameters than the carburized ones (3.7597 Å for 40 min).

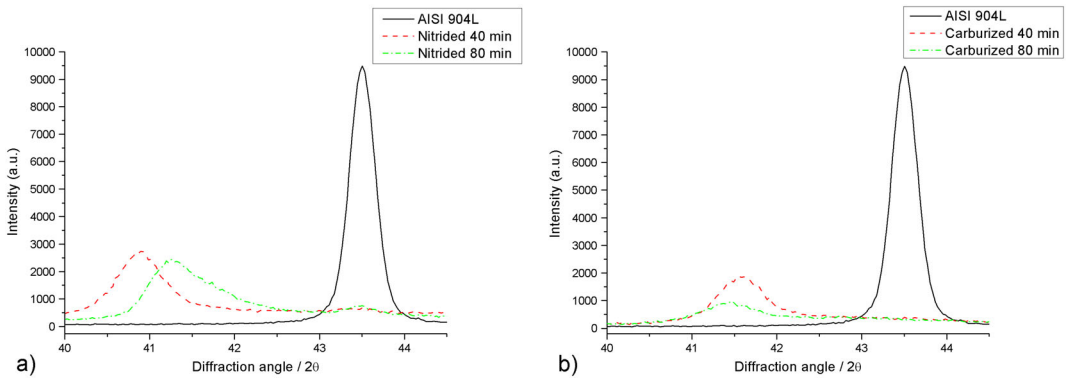


**Figure 1.** Grazing incidence X-ray diffraction diffractograms of AISI 904 L stainless steel after a) nitriding and b) carburizing processes for 40 (red dashed line) and 80 (green dash-dotted) min. The AISI 904 L diffractogram was added (black continuous line) for comparison (colors are referred only to the online version).

### Surface analysis after bombardment

In order to understand the processes involved during ion bombardment and the effect of heat treatment and the ionic collisions[18], half of the samples were covered by a thin (0.5-mm thick) foil of copper, whose specific heat capacity is 390 J/kg · K. This foil suffices to prevent the intense ion bombardment, but the heat transfer of the beam can reach the surface. Under these circumstances, it is possible to analyze the surface behavior affected solely by heat treatments. After several pulses, the side opened to ion irradiation had a gray metallic appearance, and significant roughness was detected with the naked eye. On the other hand, the side covered by the copper foil was still smooth, and in carburized samples, the dark brown color was always present. This is well represented in Fig. 2a.

In Fig. 3, the FIB/SEM images of this covered side in treated samples are shown. Craters were not detected, but a high amount of agglomerates can be found in the carburized sample (Fig. 3a). These bunches could be interpreted as graphitic structures due to the exodiffusion triggered by the heat treatment and the high mobility of carbon atoms in the steel lattice.[16] Moreover, in Fig. 3b, band slipping can be detected,[20] but there was no presence of agglomerates. In nitrided steels, the nitrogen atoms that suffered exodiffusion left the surface in gaseous form. It is important to mention that these surface effects in covered regions were the same when D or He was used as a bombarding agent.

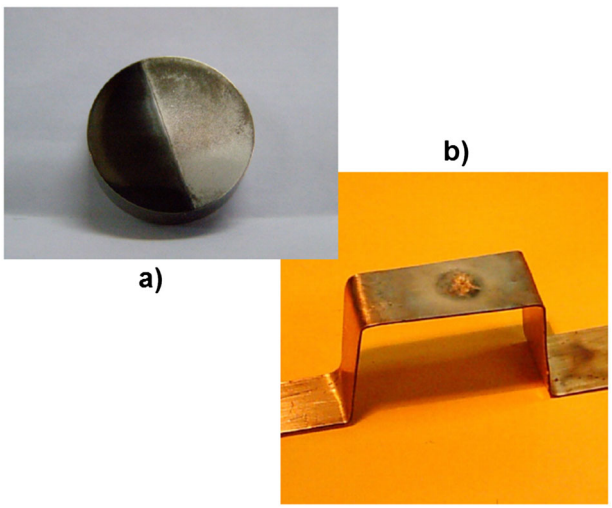


**Figure 2.** a) Carburized AISI 904 L sample showing the part hidden by the thin foil (dark brown color) and the part that suffered ion bombardment (metallic gray color). b) Bracket, made with a copper strip, used to hold the sample into the plasma focus discharge chamber. The AISI disk 'shadow' left after ion beam bombardment can be observed (the figure is in color in the online version).

The interaction of pulses with the surface has already been studied and results in a process, called thermal shock, which is a combination of ion implantation (not present when the surface was covered) and fast surface heating and cooling down.[36] In order to study the possible processes triggered, X-ray analyses (Fig. 4) were carried out. These diffractograms confirmed that in covered samples, there was a kind of disordering (the peak intensity was reduced), but the critical lost of expanding atoms (i.e. N or C) by diffusion processes was not detected.[37] A possible explanation of this effect could be the formation of amorphous regions by the fast surface heating. It is important to say that the X-ray diffraction analyses of samples showed a common behavior in respect to the peaks corresponding to the fcc crystal structure (both superaustenite and expanded austenite). Thus, taking into account such a behavior, the study concentrated on the most intense one, i.e. (111).

After this, it is worth pointing out that nitrided/carburized samples under heat treatments do not undergo important changes in their expanded structure[37] when the time of treatment is only few microseconds. Under these circumstances, only slip band reorganization and slight graphite exodiffusion were witnessed. The peak corresponding to the expanded (111) plane was fixed after ion bombardment. It is possible that copper foil did not allow the complete heat transfer that the plasma focus beam imposes, but the temperature in the sample reached high values. Furthermore, under these circumstances, D or He bombardment give same results in (111) peak position, so it is possible to say that both ions have similar thermal effects.

At this moment, it was shown that the impinging energetic ion is the main cause of surface melting and quick atom diffusion. Thus, it is interesting to see the surface morphology under ion bombardment, especially the crater's structure. The focus of the present manuscript is the role of expanded austenite as first wall in nuclear reactors. Previously, it was shown that the thermal effect (provoked in the same way when D or He is used) was not relevant in the main damaging processes. This first comparison allows only to investigate the effects produced by the ion impingement.

Carburized steel was chosen in order to study helium irradiation (Fig. 5a). In this figure, it is possible to observe several craters provoked by the high energy of the colliding ions,[18] and in the middle

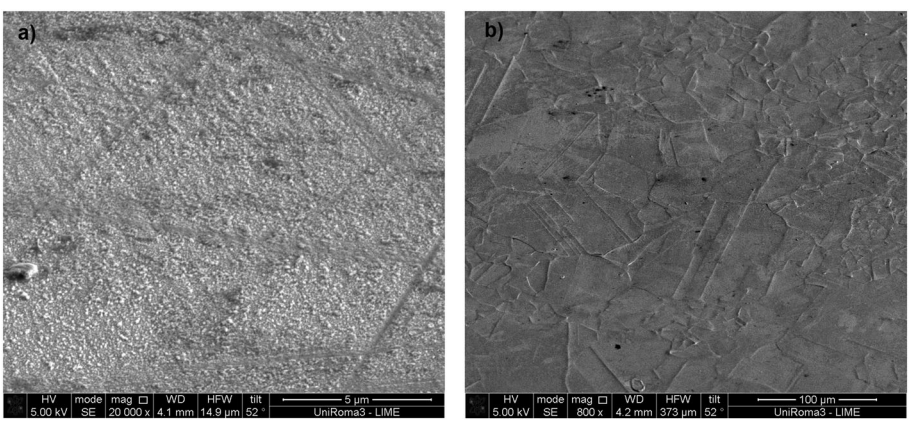


**Figure 3.** a) Carburized sample (80 min) bombarded with deuterium ions. b) Nitrided sample (80 min) bombarded with deuterium ions. Both focused ion beam/SEM images were obtained from the covered side of each sample.

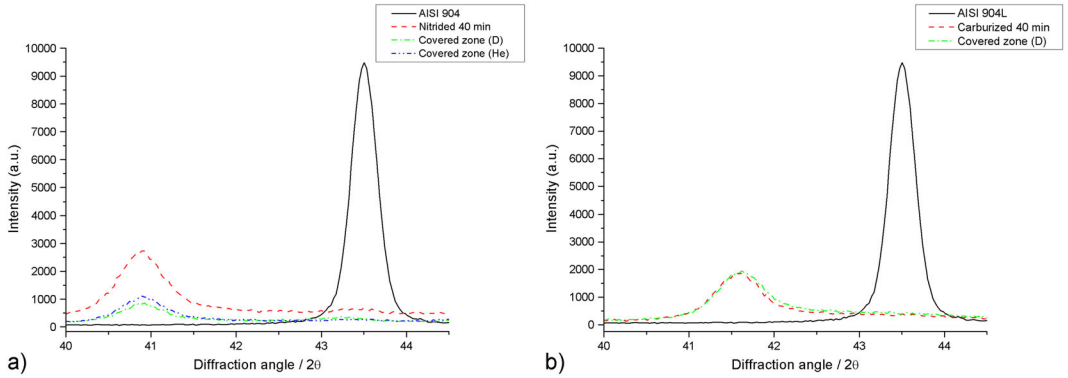


**Figure 4.** AISI 904 L stainless steel a) nitrided for 40 min and b) carburized for 40 min with and without beam irradiation on the covered zone. The black continuous line is the base material, the red dashed line is the treated sample, the green dash-dotted line is the material under deuterium irradiation, and the blue dash-dot-dotted line is the treated sample under helium irradiation (colors are referred only to the online version).

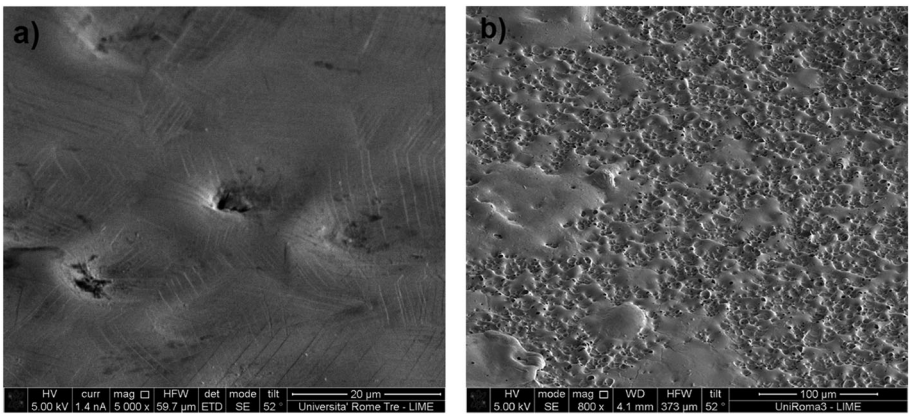


**Figure 5.** a) Surface focused ion beam/SEM image of carburized (80 min) AISI 904 L stainless steel after helium bombardment by dense plasma focus. b) Nitrided (80 min) AISI 904 L stainless steel after deuterium bombardment by dense plasma focus.

of the figure, a crater with a melted center is clearly seen. In the present paper, carburized samples (80 min) were bombarded with helium beams, and carburized samples (40 min) were bombarded with deuterium beams, so a direct comparison of surface craters in order to know the influence of the bombarding gas cannot be carried out. Furthermore, Fig. 5b depicts the surface of a nitrided sample under deuterium irradiation. It is important to say that a similar pattern was observed when helium ions were used. Regarding both figures, carburized samples are, considering only the surface region, more stable to ion bombardment than nitrided ones.[16]

Moreover, using the $Ga^+$ beam, some cross-sectional images from these craters could be obtained.[38] In Fig. 6a, it is observed that the zone under the crater is completely melted. The depth of this zone is greater than that of the range of helium ions in treated steels. Helium ions act as thermal spikes and provoke surface

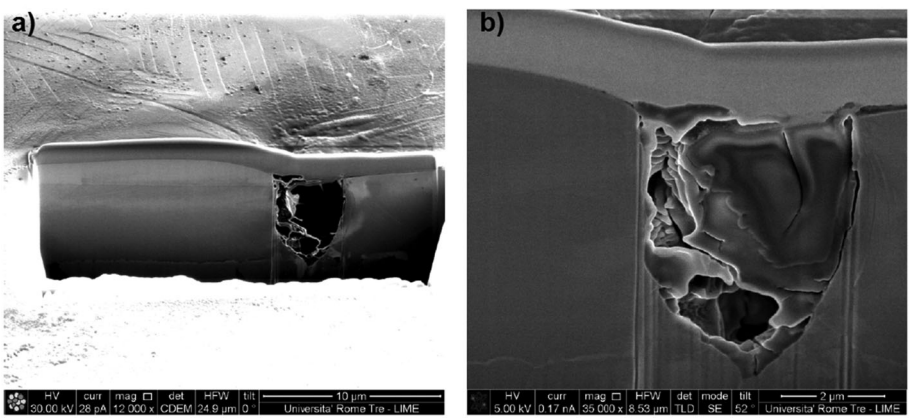


**Figure 6.** a) Cross-sectional focused ion beam/SEM image of one crater region in carburized AISI 904 L steel and b) detail of the deformed bead created by the ion implantation.

melting and quick diffusion processes.[16] Indeed, in Fig. 6b, there is, presumably, a combination of steel melting and a severe collision cascade process, so this zone had voids and an irregular shape.

These features were repeated below each crater analyzed. The zone is composed of a melted and amorphous matrix with uniform thickness (of 3-μm depth) and a melted and destroyed bead. With the EDS technique, the elemental composition of this bead can be discovered.[39] Thus, in Fig. 7, a SEM image of one melted bead could be taken (part a). EDS characterization showed that in this bead, there was no Fe (part b) or Cr (part f), both important constituents of superaustenitic stainless steels. Moreover, EDS analyses detected a concentration of S (part d) and Mn (part e) elements inside this bead structure. Pt (part c) element presence is caused by the addition of the protective layer necessary during the sputtering by $Ga^+$. Both S and Mn are elements in low proportion in AISI 904 L steel (cf. Table 1), so there might be massive Cr and Fe atom ejection.

Hence, the energetic ion impact in the surface provoked severe temperature augmentation with the consequence of surface melting[17] and atom diffusion in deeper zones (at temperatures not so elevated).[40] Also, the colliding ion itself triggered a collision cascade process[41] that ejected all the main constituents of steels, i.e. Fe and Cr and all the expansion elements (C or N), leaving solely the other steel marginal components, like S and Mn.

### Ion irradiation effects in internal layers

Not only the surface was affected by the energetic irradiation, but the internal layers were compromised too. Beneath the melted layer of 3-μm depth, there is a region where the temperatures are elevated and then diffusional effects were triggered.[42] This process provokes the loss of expanding elements (like nitrogen or carbon atoms), so expanded austenite is progressively shrunk in its lattice parameter value.[43,44] This process was observed in the whole unit cell, so the GIXRD analysis was focused again on the behavior of the (111) peak.

In the present paper, a comparison between concentration profiles before and after irradiation could not be possible. Under these experimental conditions (time processing, gas mixtures, and working pressure), nitriding and carburizing samples, before bombardment, should have a C surface concentration of ≈ 15% and N surface concentration of ≈ 25 %, according the literature.[16,18,45] After surface bombardment, it was difficult to measure the concentration profiles with depth. However, changes in (111) peak position could be a clue in order to assure a change in N or C concentration.[43] Further analyses with suitable devices should be useful to determine this.

#### *Nitrided samples*

In Fig. 8, this effect can clearly be seen in nitride superaustenitic steels after 40 min (part a) and 80 min (part b) of nitriding plasma treatment. After 20 pulses with the plasma focus device using helium or deuterium ions, the (111) peak had severely shifted to higher angular values, showing parameter lattice shrinkage.[43] This peak shifting tended towards the value of untreated stainless steel, but this peak position was not reached in any of the experiments carried out. This is a clue evidencing that there was a small amount of remaining nitrogen in the cell in order to maintain the expanded austenite phase in this region.

Nitrogen atoms could be diffused to higher depths in the samples, obeying the direction imposed by the concentration gradient.[10] On the other hand, for the same time duration considered (i.e. 40 or 80 min), it is possible to see that when using helium ions for bombardment, the loss of expansion is higher than when using deuterium ions. In Table 3, lattice parameters and relative expansions are shown in order to clarify this behavior. Perhaps, the heavier mass of helium (4.002602 u for He and 2.014102 u for D) enhanced the energy transfer to the lattice

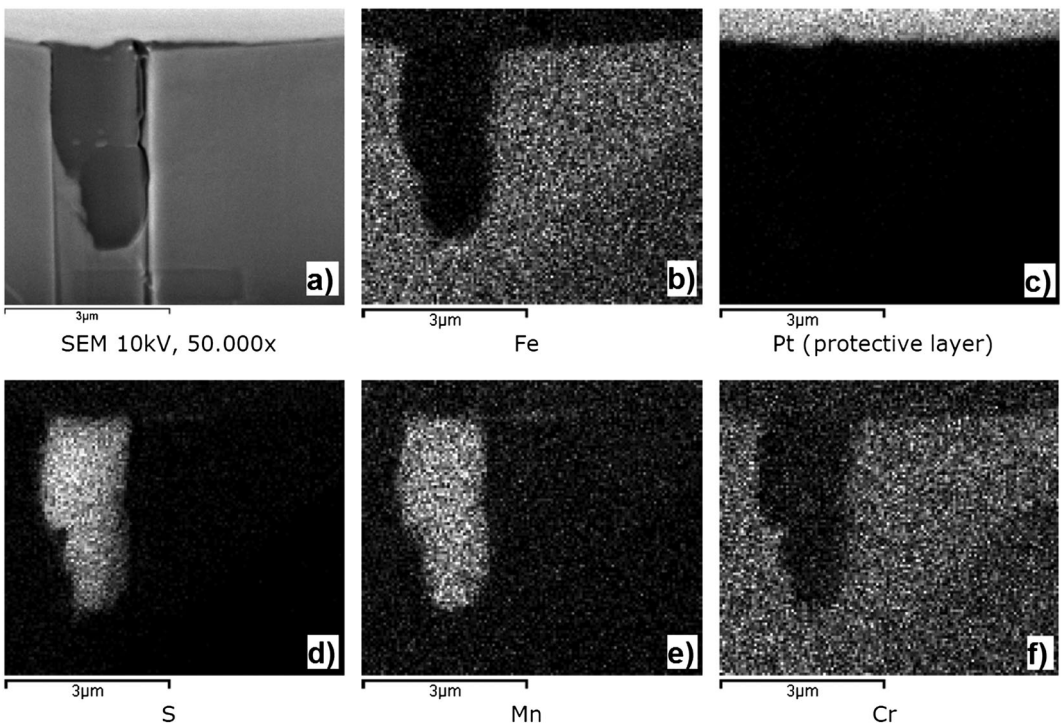


**Figure 7.** Energy-dispersive X-ray spectroscopy map mode images made in order to detect the presence of selected elements like b) Fe, c) Pt, d) S, e) Mn, and f) Cr. a) An image was obtained with SEM technique and presented the bead feature analyzed.

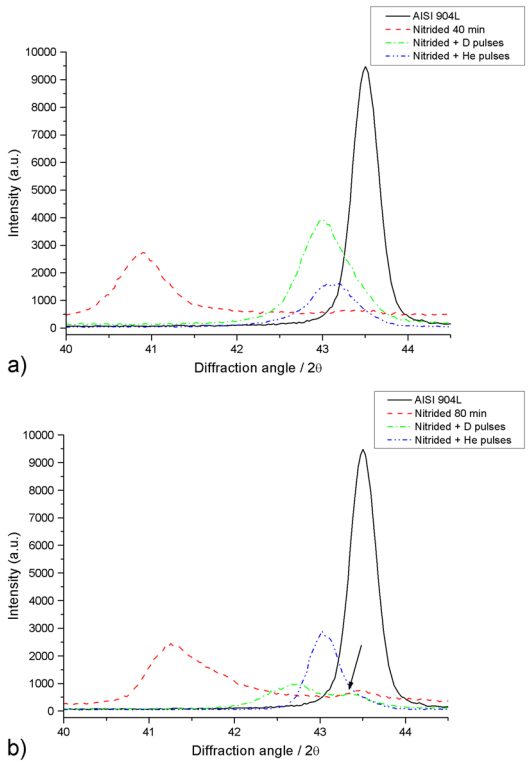


**Figure 8.** Grazing incidence X-ray diffraction spectra at 10° of incidence showing the (111) peak position of nitrided superaustenitic stainless steel before (dashed red line) and after deuterium (dash-dotted green line) and helium (dash-dot-dotted blue line) beam irradiation. AISI 904 L peak position is shown (black line) for comparative purposes. a) Diffractogram for 40 min of nitriding and b) diffractogram for 80 min of nitriding (colors are referred only to the online version).

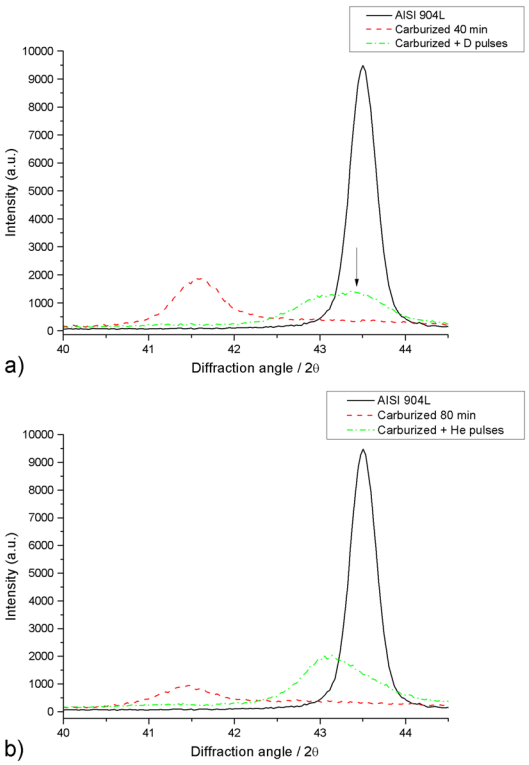


**Figure 9.** Grazing incidence X-ray diffraction diffractograms showing the (111) peaks of AISI 904 L base material (black line), carburized samples (red dashed line), and carburized samples after ion bombardment (green dash-dotted line). a) Carburized sample 40 min before and after deuterium irradiation. b) Carburized superaustenitic sample 80 min before and after helium irradiation (colors are referred only to the online version).

**Table 3.** Lattice parameter and relative expansion values of AISI 904 L samples nitrided for different amounts of time.

| | Treatment: 40 min | | Treatment: 80 min | |
|---|---|---|---|---|
| Bombardment | Lattice expansion (Å) | Relative expansion (%) | Lattice expansion (Å) | Relative expansion (%) |
| No | 3.8214 | 6.12 | 3.7824 | 5.04 |
| D ions | 3.6399 | 1.08 | 3.6662 | 1.81 |
| He ions | 3.6288 | 0.77 | 3.6356 | 0.96 |

atoms, provoking a severe collision cascade,[41] higher than the one provoked by the deuterium ions.

Another important aspect is the difference when one ion species is considered but different time durations are taken into account. When deuterium ions were selected, higher relative expansion was observed in samples nitrided for 80 min (1.81%) than those nitrided for 40 min (1.08%). This effect could be explained by the higher amount of nitrogen and the thicker nitrided case in samples treated for 80 min. On the other hand, there is not a great difference in relative expansion for the two time durations when only helium ions are considered as bombarding particles. Perhaps, this is caused by the higher mass of helium ions and the severe loss of expanding nitrogen related to the energetic collision cascade developed by them.

Moreover, an interesting phenomenon could be noted when observing Fig. 8b. When the nitrided sample is irradiated with deuterium ions, a shoulder of the (111) peak is clearly observed. An arrow points to this feature for quick identification. This peak is located at $2\theta \approx 43.3°$, and peaks in this position were already seen elsewhere.[16,18] This peak emergence was attributed to the stressed[44] steel crystallites located at the amorphous/crystal interface created in the irradiated samples. Thus, these crystallites could be explained as centers of crystalline structure nucleation with very light coarsening in a melted amorphous matrix, halted immediately by the quick drop of temperature (in only a few hundreds of nanoseconds) after melting and initialization of diffusion processes at ≈ 3-μm depth. Simultaneously, when nitrided samples under helium ion beam irradiation are analyzed, no peaks located at ≈ 43.3° can be identified. This could be provoked by the intense collision cascade developed by the helium ion impingement, which accelerates the thermal processes at high temperatures, especially in respect to the increasing and decreasing ramp rates.[17] This process is perhaps triggered in the same fashion for samples nitrided for 40 min, but the great peak breadth hides the contribution of this peak caused by the crystallites. That is, there is a peak overlapping.

**Table 4.** Lattice parameter and relative expansion values of AISI 904 L samples carburized for different amounts of time

| | Treatment: 40 min | | Treatment: 80 min | |
|---|---|---|---|---|
| Bombardment | Lattice expansion (Å) | Relative expansion (%) | Lattice expansion (Å) | Relative expansion (%) |
| No | 3.7597 | 4.41 | 3.7725 | 4.76 |
| D ions | 3.6193 | 0.51 | — | — |
| He ions | — | — | 3.6217 | 0.58 |

*Carburized samples*

In Fig. 9, the carburized samples under plasma focus irradiation (part a, 40-min carburization and deuterium bombardment, and part b, 80-min carburization and helium bombardment) and a clear lattice parameter reduction in irradiated samples can be observed. After 20 plasma focus pulses, the expanded austenite was severely damaged, and the lattice parameter shrank[42] because of interstitial carbon loss. Sample bombardment and high temperatures involved during the process developed carbon diffusion in deeper regions (in a similar way stated in the paper of Manova *et al.*[40]), so the expanded austenite is degraded, confirmed by the peak shifting to higher angular values towards the (111) AISI 904 L peak position. After this process, some carbon is located in the interstitial sites,[43] so it is possible that the loss of expansion has a limit value different than the base material one. In the work of García Molleja *et al.*,[16] it was stated that the limiting value is probably 43.3°, that is, a stressed expanded austenite structure[44] with a lattice parameter of 3.6163 Å and a relative expansion of 0.43%.

At this time, because of the selection of only a few conditions for the carburization, it was not possible to compare the different behaviors regarding different ions (deuterium or helium) used when the time duration was fixed or time durations (40 min or 80 min) used when the bombardment gas was fixed. Table 4 shows the consigned lattice expansions measured and their relative expansions associated. There was a severe loss of expansion when the carburized samples were bombarded with deuterium or helium gas, revealing a poor resistance of carburized superaustenitic steels to energetic ion bombardment.

There was a peak intensity difference between time durations when the carburized sample was not irradiated.[11] When the time duration was varied with respect to the bombarding gas, the relative expansion was similar (0.51% at 40-min carburization and deuterium bombardment and 0.58% at 80-min carburization and helium bombardment). Accordingly, following the previous considerations, the carburization time treatment did not have a huge impact on the carburized samples after bombarding. Thus, expanded austenite is severely degraded by ion bombardment, and the role of the bombarding gas was not truly appreciated. In other words, in carburized samples, severe ion bombardment reduced the expansion in the austenite in a drastic manner, regardless of the gas used.

Regarding again Fig. 9, it is worth mentioning that the peak located at 43.3° is probably present in carburized samples bombarded with deuterium atoms. Because the (111) peak after bombardment is severely shifted towards higher angular values,[34,42] peak overlapping partially hides the 43.3°-peak contribution (highlighted by the arrow in Fig. 9a). Considering the expanded austenite bombarded with helium ions, the contribution of the peak located at 43.3° is not so evident. Perhaps, the higher mass of helium ions provoked a severe collision cascade,[41] preventing the formation of stressed austenite immersed in the melted amorphous matrix. Several analyses will be conducted in order to clarify this effect.

*Comparison between nitrided and carburized samples*

Considering in a general way all the time treatments and the bombarding ions, it was possible to make a clear comparison in order to discern the role of the plasma treatment, i.e. nitriding or carburizing. Data inspection using Tables 3 and 4 suffices to obtain a clear insight.

It is customary that the expanded austenite through nitriding reaches a lattice parameter greater than that obtained from expanded austenite by carburizing.[16] It was already mentioned that the different values of solubility of carbon and nitrogen are responsible for this behavior.[34] After ion bombardment, nitrided samples had relative expansion values higher than the carburized ones, revealing that the nitriding process was the most stable. This could be explained by the different solubilities of nitrogen and carbon atoms in the austenite structure of stainless steels.[33] The ion bombardment (with helium or deuterium ions) provoked a temperature increase,[18] followed by the triggering of atom diffusion.[42] The saturation of carbon in the steel matrix was very low (with regard to nitrogen atoms), so a significant amount of these atoms were promoted to travel towards deeper regions,[40] according to the known diffusion laws.[10] This easiness of diffusion provoked the loss of expansion elements in the superficial regions (but below the melted layers) and lattice parameter shrinkage.[43] Simultaneously, the nitrogen atoms underwent the same diffusion processes, but to a lower extent, so the high lattice parameters typical of the expanded austenite were slightly reduced.

## Conclusion

In this paper, the results of an experiment involving superaustenitic AISI 904 L stainless steel nitrided/carburized for different amounts of time (40 and 80 min) with pulsed plasma glow discharges, using a mixture of gases containing molecular nitrogen/methane, were discussed. In order to study their surface structures and their stability, these samples were subjected to severe ion irradiation (20 pulses of helium/deuterium) using a plasma focus device.

Several characterization techniques were used to reach the following conclusions:

- Nitrogen and carbon atoms were lodged in the fcc interstitial sites in order to develop the structure called expanded austenite. In carburized samples, the expansion grew with time processing, but the opposite trend was detected in nitrided samples, because of the possible formation of nitride nanoagglomerates on the surface.
- Expanded austenite caused by nitriding had higher lattice parameters than the expanded austenite obtained by carburizing, due to the different solubility values between N and C, respectively.
- The treated surface was stable in its crystalline configuration only when a heat contribution (thousands of degrees for

microseconds) was applied in these regions. Moreover, the expanded austenite stability was modified when the surface suffered ion bombardment.

- Ion impingement provoked surface melting and amorphization in the first ≈ 3 μm of depth. Beneath the craters developed by the ion collision, a melted and severely damaged bead was detected. Intense collision cascade diffused the main steel components (i.e. Fe and Cr), and only the minor alloying remained (i.e. S and Mn).
- Layers at ≈ 3-μm depth engaged in diffusion processes because of thermal effects, so the expanded austenite was reduced progressively in terms of its lattice parameter.
- In nitrided samples, helium bombardment provoked a high loss of expansion. This loss was more accentuated in samples nitrided for 40 min. Treated samples bombarded with deuterium ions developed a diffraction peak located at ≈ 43.3°, because of the formation of crystallites of stressed austenite near the melted region. The thermal gradients were responsible for the development of this nucleation of crystalline grains and their slight coarsening.
- In carburized samples, expanded austenite stability was lower than in nitrided samples. Moreover, time treatment did not have a relevant role in affecting the stability. It is important to mention that carburized samples under deuterium bombardment developed a diffraction peak located at ≈ 43.3° because of stressed austenite formation.

**Acknowledgements**

The research work was assisted through PICT 2008-0374 of ANPCyT (Argentina) and project IT/10/06 of the 'Programa de Cooperación Bilateral Científico-Tecnológico Argentino-Italiano MINCyT-MAE'. The authors are grateful to Daniel Castellani, Daniele de Felicis, and Javier Cruceño for their assistance and equipment maintenance. Conicet (Argentina), Universidad de Córdoba (Spain), Universidad de Investigación de Tecnología Experimental Yachay (Ecuador) and CNRS (France), as funding institutions, are deeply acknowledged.

## References

[1] H.K. Lo, C.H. Shek, J.K.L. Lai, Recent developments in stainless steels, *Mater Sci Eng* **2009**, *R 65*, 39–104.
[2] J.K.L. Lai, K.H. Lo, C.H. Shek, *Stainless Steels: An Introduction and Their Recent Developments, Bentham Books*, Sharjah-Oak, Park-Bussum, **2013**.
[3] Y. Cao, M. Norell, Role of nitrogen uptake during the oxidation of 304 L and 904 L austenitic stainless steels, *Oxid Met* **2013**, *80*, 479–491.
[4] R. Cortés, J. Villanueva, E. Ponce, M. Rojas, E. Rojas, *Estudio de la Soldabilidad y Corrosión del Acero Inoxidable AISI 904L con los Agentes Utilizados en la Lixivación del Cobre12*, Revista Facultad de Ingeniería, U.T.A. (Chile), **2004**, pp. 43–56.
[5] F.A.P. Fernandes, S.C. Heck, R.G. Pereira, C.A. Picon, P.A.P. Nascente, L. C. Casteletti, Ion nitriding of a superaustenitic stainless steel: wear and corrosion characterization, *Surf Coat Technol* **2010**, *204*, 3087–3090.
[6] A. Matthews, A. Leyland, B. Dorn, P.R. Stevenson, M. Bin-Sudin, C. Rebholz, A. Voevodin, J. Schneider, Hybrid techniques in surface engineering, *J Vac Sci Technol* **1995**, *A 13*, 1202.
[7] A. Leyland, D.B. Lewis, P.R. Stevenson, A. Matthews, Low temperature plasma diffusion treatment of stainless steels for improved wear resistance, *Surf Coat Technol* **1993**, *62*, 608–617.
[8] Y. Sun, Kinetics of low temperature plasma carburizing of austenitic stainless steels, *J Mater Process Technol* **2005**, *168*, 189–194.
[9] A. Çelik, M. Karakan, A. Alsaran, I. Efeoglu, The investigation of structural, mechanical and tribological properties of plasma nitrocarburized AISI 1020 steel, *Surf Coat Technol* **2005**, *200*, 1926–1932.
[10] T. Czerwiec, N. Renevier, H. Michel, Low temperature plasma-assisted nitriding, *Surf Coat Technol* **2000**, *131*, 267–277.
[11] J. García Molleja, L. Nosei, J. Ferrón, E. Bemporad, J. Lesage, D. Chicot, J. Feugeas, Characterization of expanded austenite developed on AISI 316 L stainless steel by plasma carburization, *Surf Coat Technol* **2010**, *204*, 3750–3759.
[12] S. Latha, M.D. Mathew, P. Parameswaran, K. Bhanu Sankara Rao, S. L. Mannan, Thermal creep properties of alloy D9 stainless steel and 316 stainless steel fuel clad tubes, *Int J Pres Ves Pip* **2008**, *85*, 866–870.
[13] G. Amarendra, B.K. Panigrahi, S. Abhaya, C. David, R. Rajaraman, K.G. M. Nair, C.S. Sundar, B. Raj, Positron beam studies of void swelling in ion irradiated Ti-modified stainless steels, *Appl Surf Sci* **2008**, *255*, 139–141.
[14] L. Rico, B.J. Gómez, J. Feugeas, O. de Sanctis, Crystallization of amorphous zirconium thin film using ion implantation by a plasma focus of 1 kJ, *Appl Surf Sci* **2007**, *254*, 193–196.
[15] M. Akel, S. Al-Hawat, S.H. Saw, S. Lee, Numerical experiments on oxygen soft X-ray emissions from low energy plasma focus using Lee model, *J Fusion Energy* **2010**, *29*, 233–231.
[16] J. García Molleja, M. Milanese, M. Piccoli, R. Moroso, J. Niedbalski, L. Nosei, J. Bürgi, E. Bemporad, J. Feugeas, Stability of expanded austenite, generated by ion carburizing and ion nitriding of AISI 316 L SS, under high temperature and high energy pulsed ion beam irradiation, *Surf Coat Technol* **2013**, *218*, 142–151.
[17] V.N. Pimenov, E.V. Demina, S.A. Maslyaev, L.I. Ivanov, V.A. Gribkov, A. V. Dubrovsky, U. Ugaste, T. Laas, M. Scholz, R. Miklaszewski, B. Kolman, A. Tartari, Damage and modification of materials produced by pulsed ion and plasma streams in dense plasma focus device, *Nukleonika* **2008**, *53*, 111–121.
[18] J. Feugeas, L. Rico, L. Nosei, B. Gómez, E. Bemporad, J. Lesage, J. Ferrón, Austenite modification of AISI 316 L SS by pulsed nitrogen ion beams generated in dense plasma focus discharges, *Surf Coat Technol* **2010**, *204*, 1193–1199.
[19] C.X. Li, T. Bell, Sliding wear properties of active screen plasma nitrided 316 austenitic stainless steel, *Wear* **2004**, *256*, 1144–1152.
[20] L. Nosei, M. Ávalos, B.J. Gómez, L. Náchez, J. Feugeas, Stability under temperature of expanded austenite developed on stainless steel AISI 316 L by ion nitriding, *Thin Solid Films* **2004**, *468*, 134–141.
[21] M. Milanese, R. Moroso, J. Pouzo, Dynamics of the ionizing and magnetic fronts in the radial compression stage of a DPF current sheath, *IEEE Trans Plasma Sci* **1993**, *21*, 373–377.
[22] T. Haruki, H.R. Yousefi, K. Masugata, J.-I. Sakai, Y. Mizuguchi, N. Makino, H. Ito, Simulation of high-energy particle production through sausage and kink instabilities in pinched plasma discharges, *Phys Plasmas* **2006**, *13*, 082106.
[23] M.M. Milanese, R.L. Moroso, The first stages of the discharge in a low-energy dense plasma focus, *IEEE Trans Plasma Sci* **2005**, *33*, 1658–1661.
[24] G. Sánchez, G. Grigioni, J. Feugeas, Thermal effect of ion implantation with ultra-short ion beams, *Surf Coat Technol* **1995**, *70*, 181–186.
[25] J. García Molleja, Caracterización de austenite expandida generada por cementación iónica de aceros inoxidables. Estudio de la estabilidad frente a la irradiación con haces de iones ligeros energéticos, PhD Thesis, Universidad Nacional de Rosario, Argentina, **2012**
[26] R.L. Klueh, D.S. Gelles, S. Jitsukawa, A. Kimura, G.R. Odette, B. van der Schaaf, M. Victoria, Ferritic/martensitic steels – overview of recent results, *J Nucl Mater* **2002**, *307-311*, 455–465.
[27] X. Song, K.B. Yeap, J. Zhu, J. Belnoue, M. Sebastiani, E. Bemporad, K. Y. Zeng, A.M. Korsunsky, Residual stress measurement in thin films using the semi-destructive ring-core drilling method using focused ion beam, *Procedia Eng* **2011**, *10*, 2190–2195.
[28] F.J. Baldenebro-López, C.D. Gómez-Esparza, R. Corral-Higuera, S. P. Arredondo-Rea, M.J. Pellegrini-Cervantes, J.E. Ledezma-Sillas, R. Martínez-Sánchez, J.M. Herrera-Ramírez, Influence of size on the microstructure and mechanical properties of an AISI 304 L stainless steel – a comparison between bulk and fibers, *Materials* **2015**, *8*, 451–461.
[29] F.C. Nascimento, C.E. Foerster, S.L.R. da Silva, C.M. Lepienski, C.J. M. Siqueira, C.A. Júnior, A comparative study of mechanical and tribological properties of AISI-304 and AISI-316 submitted to glow discharge nitriding, *Mater Res* **2009**, *12*, 173–180.
[30] A.M. Abd El-Rahman, S.H. Mohamed, M.R. Ahmed, E. Richter, F. Prokert, Nitrocarburizing of AISI-304 stainless steel using high-voltage plasma immersion ion implantation, *Nucl Instrum Methods Phys Res* **2009**, *B 267*, 1792–1796.

  

[31] C.E. Foerster, A. Assmann, S.L.R. da Silva, F.C. Nascimento, C. M. Lepienski, J.L. Guimarães, A.L. Chinelatto, AISI 304 nitrocarburized at low temperature: mechanical and tribological properties, *Surf Coat Technol* **2010**, *204*, 3004–3008.

[32] J. Feugeas, B. Gómez, A. Craievich, Ion nitriding of stainless steels. Real time surface characterization by synchrotron X-ray diffraction, *Surf Coat Technol* **2002**, *154*, 167–175.

[33] L. Gil, S. Brühl, L. Jiménez, O. Leon, R. Guevara, M.H. Staia, Corrosion performance of the plasma nitrided 316 L stainless steel, *Surf Coat Technol* **2006**, *201*, 4424–4429.

[34] D.L. Williamson, O. Ozturk, R. Wei, P. Wilbur, Metastable phase formation and enhanced diffusion in f.c.c. alloys under high dose, high flux nitrogen implantation at high and low ion energies, *Surf Coat Technol* **1994**, *65*, 15–23.

[35] M. Tsujikawa, D. Yoshida, N. Yamauchi, N. Ueda, T. Sone, S. Tanaka, Surface material design of 316 stainless steel by combination of low temperature carburizing and nitriding, *Surf Coat Technol* **2005**, *200*, 507–511.

[36] G. Sánchez, J. Feugeas, The thermal evolution of targets under plasma focus pulsed ion implantation, *J Phys D Appl Phys* **1997**, *30*, 927–936.

[37] B. Sartowska, J. Piekoszewski, L. Waliś, J. Stanisławski, L. Nowicki, R. Ratajczak, M. Kopcewicz, J. Senatorski, Thermal stability of the phases formed in the near surface layers of unalloyed steels by nitrogen pulsed plasma treatment, *Vacuum* **2007**, *81*, 1188–1190.

[38] E. Bemporad, M. Sebastiani, M.H. Staia, E. Puchi Cabrera, Tribological studies on PVD/HVOF duplex coatings on Ti6Al4V substrate, *Surf Coat Technol* **2008**, *203*, 566–571.

[39] K. Chakrabarti, J.J. Jeong, S.K. Hwang, Y.C. Yoo, C.M. Lee, Effects of nitrogen flow rates on the growth morphology of TiAlN films prepared by an rf-reactive sputtering technique, *Thin Solid Films* **2002**, *406*, 159–163.

[40] D. Manova, S. Mändl, H. Neumann, B. Rauschenbach, Influence of grain size on nitrogen diffusivity in austenitic stainless steels, *Surf Coat Technol* **2007**, *201*, 6686–6689.

[41] M.V. Roshan, R.S. Rawat, A.R. Babazadeh, M. Emami, S.M. Sadat Kiai, R. Verma, J.J. Lin, A.R. Talebitaher, P. Lee, S.V. Springham, High energy ions and energetic plasma irradiation effects on aluminium in a Filippov-type plasma focus, *Appl Surf Sci* **2008**, *255*, 2461–2465.

[42] G. Murtaza, S.S. Hussain, M. Sadiq, M. Zakaullah, Plasma focus assisted carburizing of aluminium, *Thin Solid Films* **2009**, *517*, 6777–6783.

[43] N.N. Rammo, O.G. Abdulah, A model for the prediction of lattice parameters of iron-carbon austenite and martensite, *J Alloys Compd* **2006**, *420*, 117–120.

[44] A.H. Heuer, F. Ernst, H. Kahn, A. Avishai, G.M. Michal, D.J. Pitchure, R. E. Ricker, Interstitial defects in 316 L austenitic stainless steel containing "colossal" carbon concentrations: an internal friction study, *Scripta Mater* **2007**, *56*, 1067–1070.

[45] J.P. Rivière, C. Templier, A. Declémy, O. Redjal, Y. Chumlyakov, G. Abrasonis, Microstructure of expanded austenite in ion-nitrided AISI 316 L single crystals, *Surf Coat Technol* **2007**, *201*, 8210–8214.